Atmos. Chem. Phys. Discuss., doi:10.5194/acp-2016-303, 2016
Manuscript under review for journal Atmos. Chem. Phys.
Published: 10 May 2016

Atmospheric Chemistry and Physics Discussions

Seasonal Variability of Stratospheric Methane: Implications for Constraining Tropospheric Methane Budgets Using Total Column Observations

K. M. Saad[1], D. Wunch[1,2], N. M. Deutscher[3,4], D. W. T. Griffith[3], F. Hase[5], M. De Mazière[6], J. Notholt[4], D. F. Pollard[7], C. M. Roehl[1], M. Schneider[5], R. Sussmann[8], T. Warneke[4], and P. O. Wennberg[1]

[1]California Institute of Technology, Pasadena, California, USA
[2]University of Toronto, Toronto, Ontario, Canada
[3]University of Wollongong, Wollongong, NSW, Australia
[4]University of Bremen, Bremen, Germany
[5]Karlsruhe Institute of Technology, IMK-ASF, Karlsruhe, Germany
[6]Royal Belgian Institute for Space Aeronomy, Brussels, Belgium
[7]National Institute of Water and Atmospheric Research, Omakau, New Zealand
[8]Karlsruhe Institute of Technology, IMK-IFU, Garmisch-Partenkirchen, Germany

Correspondence to: K. M. Saad (katsaad@caltech.edu)

Abstract. Global and regional methane budgets are uncertain due to the large number of highly variable sources. Current estimates are derived by bridging emissions inventories with atmospheric observations using chemical transport models. This approach requires accurately simulating advection and chemical loss to produce valid distributions of methane concentrations resulting from surface fluxes when assimilating total column measurements. To assess the impact of model stratospheric errors on inversions that assimilate total columns, we compare the agreement between Total Carbon Column Observing Network (TCCON) and GEOS-Chem total and tropospheric column-averaged mole fractions of methane. We find both a mismatch in the Northern Hemisphere stratospheric contribution that increases as the tropopause altitude decreases and a temporal phase lag in the model's tropospheric seasonality driven by transport errors. These tropospheric errors particularly compensate the stratospheric discrepancies between measurements and models, thereby producing agreement in the total columns masking inconsistencies in methane vertical profiles. These errors alias into source attribution resulting from model inversions. We estimate that the tropospheric time lag leads to large errors in posterior wetland emissions in the high latitudes of the Northern Hemisphere.

1 Introduction

Identifying the processes that have driven changes in atmospheric methane (CH_4), a potent radiative forcing agent and major driver of tropospheric oxidant budgets, is critical for understanding future impacts on the climate system. Methane's growth rate, which had been decreasing through the 1990s from about 10 to 0 ppb per year, began to increase again in 2006 and over the past decade has averaged 5 ppb per year (Dlugokencky et al., 2011). Developing robust constraints on the global CH_4

Atmos. Chem. Phys. Discuss., doi:10.5194/acp-2016-303, 2016
Manuscript under review for journal Atmos. Chem. Phys.
Published: 10 May 2016

Atmospheric Chemistry and Physics Discussions

budget is integral for understanding which processes produced these decadal trends (e.g., Bergamaschi et al., 2013; Wecht et al., 2014a, b; Turner et al., 2015).

One common approach to quantifying changes in the spatial distribution of sources incorporates surface fluxes estimated by bottom-up inventories as boundary conditions for a chemical transport model (CTM). The modeled CH_4 concentrations are compared to observations within associated grid boxes, and prior emissions are scaled to minimize differences with measured dry-air mole fractions (DMFs), producing posterior estimates. This method assumes that each source's relative contribution to a given grid box's concentration are known at any point in time. The accuracy of these optimized emissions depends on how well the CTM simulates atmospheric transport and CH_4 sinks, which are generally prescribed.

Pressure-weighted total column-averaged DMFs (X_{gas}) provide a relatively new constraint and have previously been shown to improve estimates of regional and interhemispheric gradients in trace gases (Stephens et al., 2007; Yang et al., 2007). Fourier transform infrared spectrometers can measure CH_4 DMFs (X_{CH_4}) from ground-based sites, such as those in the Total Carbon Column Observing Network (TCCON) and Network for the Detection of Atmospheric Composition Change (NDACC), and satellites, including SCanning Imaging Absorption spectroMeter for Atmospheric CartograpHY (SCIAMACHY) (Bergamaschi et al., 2007), Greenhouse gases Observing SATellite (GOSAT) (Parker et al., 2011), and the upcoming TROPOspheric Monitoring Instrument (TROPOMI) (Butz et al., 2012). These observations complement surface measurements because they add information about the vertically-averaged profile and are sensitive in the free troposphere (Yang et al., 2007). Additionally, they complement aircraft observations by measuring trace gases at higher temporal frequency. Satellite measurements also add global coverage that can fill in gaps where in situ observations are sparse. Fraser et al. (2013) found that GOSAT CH_4 columns reduced posterior emissions uncertainties by up to 45% compared to inversions that only assimilated surface data. Wecht et al. (2014b) determined that TROPOMI's global daily measurements will provide a constraint on California's CH_4 emissions similar to CalNex aircraft observations (Santoni et al., 2014; Gentner et al., 2014).

Incorporating total columns can also be used to diagnose systematic issues with model transport. Comparing carbon dioxide (CO_2) from TCCON and TransCom (Baker et al., 2006), Yang et al. (2007) found that most TransCom models lack sufficiently strong vertical transport from the planetary boundary layer (PBL) to the mixed layer, thereby dampening the seasonal cycle amplitude of CO_2 in the free troposphere. More recent studies attribute to model transport errors the tendency of simulated CH_4 in the Southern Hemisphere to be higher at the surface than the free troposphere, in contrast with measurements (Patra et al., 2011; Fraser et al., 2011).

Tropospheric CH_4 typically does not vary radically with height above the PBL; above the tropopause, however, the vertical profile of CH_4 exhibits a rapid decline with altitude as a result of its oxidation. Fluctuations in stratospheric dynamics, including the height of the tropopause, change the contribution of the stratosphere to the total column. CH_4 profiles with similar tropospheric values can thus have significant differences in X_{CH_4} (Saad et al., 2014; Washenfelder et al., 2003; Wang et al., 2014).

Insofar as simulations replicate seasonal and zonal variability of stratospheric CH_4 loss, tropopause heights, and vertical exchange across the upper troposphere and lower stratosphere (UTLS), posterior flux estimates from inversions incorporating X_{CH_4} measurements would not be sensitive to stratospheric processes. However, most models do not accurately represent

Atmos. Chem. Phys. Discuss., doi:10.5194/acp-2016-303, 2016
Manuscript under review for journal Atmos. Chem. Phys.
Published: 10 May 2016

Atmospheric Chemistry and Physics Discussions

Figure 1. Map of TCCON sites used in this analysis. Site colors are on a spectral color scale in order of latitude, with Northern Hemisphere sites designated by cool colors and Southern Hemisphere sites designated by warm colors.

stratospheric transport, producing low age of air values and zonal gradients in the subtropical lower stratosphere that are less steep than observations (Waugh and Hall, 2002). As temporal and spatial biases in a model's vertical profile will alias into posterior emissions, inversions that incorporate total column measurements must ensure that the stratosphere is sufficiently well described so as to not introduce spurious seasonal, zonal and interhemispheric trends in $\mathrm{CH_4}$ concentrations and consequently emissions.

In this analysis, we identify systematic model biases in the seasonal cycle and spatial distribution of $\mathrm{CH_4}$ by comparing TCCON total and tropospheric columns (Saad et al., 2014) to vertically integrated profiles derived from the GEOS-Chem CTM (Bey et al., 2001; Wang et al., 2004; Wecht et al., 2014a). We assess the impact of errors in the characterization of stratospheric processes on assimilation of $X_{\mathrm{CH_4}}$ and resulting posterior emissions estimates. In Section 2 we describe the TCCON column measurements and GEOS-Chem set up and characteristics. In Section 3 we present the results of the measurement-model comparison. In Section 4 we compare the base case simulation to one in which emissions fluxes do not vary within each year and quantify the sensitivity of source attribution of the biggest seasonal emissions sector, wetlands, to the tropospheric seasonal delay.

2 Methods

2.1 Tropospheric Methane Columns

TCCON has provided precise measurements of $X_{\mathrm{CH_4}}$ and other atmospheric trace gases for over ten years (Wunch et al., 2011a). Developed to address open questions in carbon cycle science, the earliest sites are located in Park Falls, Wisconsin, United States and Lauder, New Zealand at $45°$ North and South, respectively. Since 2004, the ground-based network of Fourier transform spectrometers has expanded greatly.

Atmos. Chem. Phys. Discuss., doi:10.5194/acp-2016-303, 2016
Manuscript under review for journal Atmos. Chem. Phys.
Published: 10 May 2016

Atmospheric Chemistry and Physics Discussions

The tropospheric CH_4 columns ($X^t_{CH_4}$) are derived by the hydrogen fluoride (HF) proxy method described in Saad et al. (2014), which uses the relationship between CH_4 and HF in the stratosphere, derived from ACE-FTS satellite measurements (Bernath, 2005; De Mazière et al., 2008; Mahieu et al., 2008; Waymark et al., 2014), to calculate the stratospheric contribution to X_{CH_4}. Tropospheric columns have been shown to represent the magnitude and seasonality of in situ measurements (Saad et al., 2014; Washenfelder et al., 2003; Wang et al., 2014). The $X^t_{CH_4}$ used in this analysis have been processed consistently with the GGG2014 TCCON products, with airmass dependence and calibration factors calculated for and applied to $X^t_{CH_4}$ (Wunch et al., 2010, 2015). With the exception of Eureka and Sodankylä, which are highly influenced by the stratospheric polar vortex, all TCCON sites that provide measurements before December 2011 are included in this analysis (Fig. 1). Table 1 lists locations and data collection start dates for each of the sites.

Table 1. TCCON sites, coordinates, altitudes, start date of measurements and locations used in this analysis.

Site	Latitude (°)	Longitude (°)	Elevation (km)	Start Date	Location
Bialystok	53.2	23.0	0.18	Mar 2009	Bialystok, Poland
Bremen	53.1	8.9	0.03	Jan 2007	Bremen, Germany
Karlsruhe	49.1	8.4	0.11	Apr 2010	Karlsruhe, Germany
Orleans	48.0	2.1	0.13	Aug 2009	Orleans, France
Garmisch	47.5	11.1	0.75	Jul 2007	Garmisch, Germany
Park Falls	45.9	-90.3	0.47	Jan 2005	Park Falls, WI, USA
Lamont	36.6	-97.5	0.32	Jul 2008	Lamont, OK, USA
JPL	34.2	-118.2	0.39	Jul 2007	Pasadena, CA, USA
Saga	33.2	130.3	0.01	Jul 2011	Saga, Japan
Izaña	28.3	-16.5	2.37	May 2007	Tenerife, Canary Islands
Darwin	12.4	130.9	0.03	Aug 2005	Darwin, Australia
Réunion Island	-20.9	55.5	0.09	Sep 2011	Saint-Denis, Réunion
Wollongong	-34.4	150.9	0.03	Jun 2008	Wollongong, Australia
Lauder	-45.0	169.7	0.37	Jan 2005	Lauder, New Zealand

2.2 GEOS-Chem Model

Model comparisons use the offline CH_4 GEOS-Chem version 9.02 at $4 \times 5°$ horizontal resolution on a reduced vertical grid (47L). CH_4 loss is calculated on 60 minute intervals and is set by 3D monthly fields: hydroxyl radical (OH) concentrations in the troposphere and parameterized CH_4 loss rates per unit volume in the stratosphere. Emissions are released at 60-minute time steps and are split between 10 sectors: gas and oil, coal, livestock, waste, biofuel, other anthropogenic, and other natural emissions annual values; rice agriculture and wetland monthly values; and biomass burning daily values using GFED3 emissions estimates. Loss via soil absorption, set annually, is subtracted from the total emissions at each time step.

Atmos. Chem. Phys. Discuss., doi:10.5194/acp-2016-303, 2016
Manuscript under review for journal Atmos. Chem. Phys.
Published: 10 May 2016

Atmospheric Chemistry and Physics Discussions

2.2.1 Model Set Up

We initialized zonal CH_4 distributions with GGG2014 data version a priori profiles (Wunch et al., 2015) produced at horizontal grid centers, which we adjusted vertically to match the zonally averaged daily mean GEOS5 tropopause. The model was run from December 2003, the first month in which GEOS5 meteorological data was available, to June 2004, the beginning of the TCCON time series; we then ran the model repeatedly over the June 2004-May 2005 time frame, which allowed us to make comparisons with the TCCON data at Park Falls and Lauder, until CH_4 concentrations reached equilibrium. A number of perturbation experiments were run in this way to quantify the sensitivity of CH_4 distribution and seasonality to the offline OH fields, prescribed emissions, and tropopause levels (Table 2). These model experiments are described in greater detail in Appendix A1.

Using CH_4 fields for 1 January 2005 from the equilibrium simulation as initial conditions, model daily mean CH_4 mole fractions were computed through 2011. In addition to the default emissions scheme, an aseasonal simulation setup, in which rice, wetland, and biomass burning emissions were disabled and aseasonal emissions scaled up such that total annual zonal fluxes approximate those in the base simulation, was similarly run to equilibrium and initial conditions for the 2005-2011 run.

For comparisons with column measurements, model vertical profiles were smoothed with corresponding TCCON CH_4 averaging kernels and daily median scaled priors using daily mean surface pressures and solar zenith angles for each site, following the methodology in Rodgers and Connor (2003) and Wunch et al. (2010). Tropospheric columns were integrated in the same manner as the total columns up to the grid level completely below the daily mean tropopause, consistent with how GEOS-Chem partitions the atmosphere in the offline CH_4 simulation. To test the dependence of our results to the chosen vertical integration level, tropospheric columns were also calculated assuming the tropopause was one and two grid cells above this level. While $X^t_{CH_4}$ changed slightly, shifting the tropopause did not alter the findings discussed in this paper. The stratospheric contribution is calculated as the residual between the tropospheric and total columns. A description of the model smoothing methodology and assumptions is provided in Appendix A3.

2.2.2 Model Features

The seasonal amplitude of the differences between base and aseasonal simulations are small for all vertical levels in the Southern Hemisphere (Fig. 2). In the Northern Hemisphere, however, the difference in the amplitude is much larger and

Table 2. Table of Sensitivity Experiments

Run Name	Description	CH_4 Lifetime (years)	Final CH_4 Burden (Tg)
Base	Default OH and Emissions	9.55	4825
Aseasonal	Constant Monthly Emission Rates	9.57	4872
Updated OH	Monthly OH fields from Standard Chemistry + Biogenic VOCS	8.53	4828

Atmos. Chem. Phys. Discuss., doi:10.5194/acp-2016-303, 2016
Manuscript under review for journal Atmos. Chem. Phys.
Published: 10 May 2016

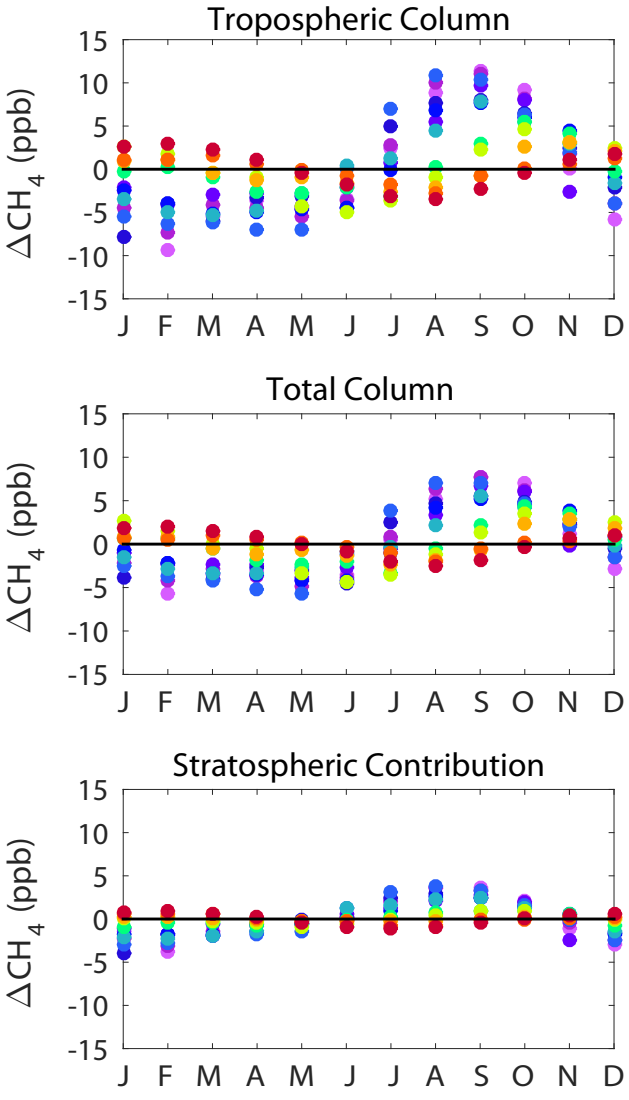

Figure 2. Seasonality of the difference between base and aseasonal CH_4 for tropospheric, total and stratospheric contribution to total columns. Site colors are as in Fig. 1.

primarily impacts the troposphere. The insensitivity of the stratosphere to emissions seasonality is due to the common source of stratospheric air in the tropics (Boering et al., 1995) and the loss of seasonal information as the age of air increases.

Due to the relatively short photochemical lifetime of CH_4 in the stratosphere, stratospheric CH_4 concentrations stabilize much more quickly than in the troposphere (Fig. 3a). This rapid response time of the stratosphere occurs regardless of perturbations to the troposphere, such as emissions seasonality (Fig. 3b) or tropospheric OH fields (Fig. 3c). In both hemispheres the differences between the base and experimental simulations asymptotically approach steady state with seasonal variability

Atmos. Chem. Phys. Discuss., doi:10.5194/acp-2016-303, 2016
Manuscript under review for journal Atmos. Chem. Phys.
Published: 10 May 2016

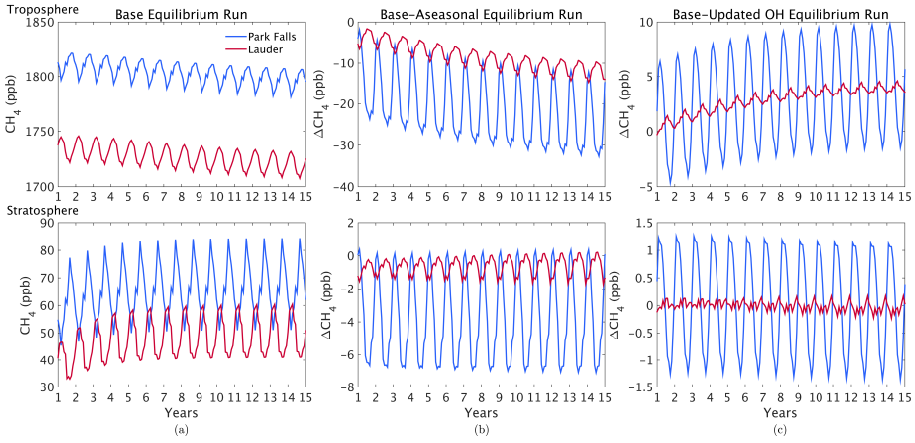

Figure 3. Smoothed daily mean CH_4 DMFs at Park Falls (blue) and Lauder (red) for (a) base equilibrium simulation and the difference between the base and (b) aseasonal and (c) updated OH simulations.

over a decade in the troposphere, but oscillate seasonally around a constant mean in the stratosphere. Stratospheric differences between simulations are considerably lower than the seasonal amplitude of the base run: within six and one ppb, respectively, versus a seasonal amplitude of 15 ppb at Park Falls. By contrast, $X^t_{CH_4}$ have differences within 30 and 10 ppb, respectively, versus a seasonal amplitude of 10 ppb at Park Falls. The stratosphere at Lauder is even less sensitive to tropospheric perturbations.

3 Measurement-Model Comparison

The TCCON daily median and GEOS-Chem daily mean CH_4 DMFs are highly correlated for both the tropospheric and total columns, with R^2 values of 0.89 and 0.86 for their respective least squares linear regressions (Fig. 4, top). However, the tropospheric slope is less than one while the total column slope is greater than one, indicating that the temporal variability differs in the troposphere and stratosphere. While no hemispheric difference is apparent for either $X^t_{CH_4}$ or X_{CH_4}, the stratospheric relationship between the measurements and model bifurcate between the Northern and Southern Hemispheres, as evidenced by the lower correlation coefficient of 0.75 (Fig. 4c, top). TCCON and GEOS-Chem are consistent across the Southern Hemisphere sites; the slope, intercept and correlation coefficient are 1.1±0.020, 6, and 0.84, respectively. By contrast, in the Northern Hemisphere the TCCON stratospheric contribution is less than that of GEOS-Chem, the linear regression has a slope of 0.50±0.012, and the relationship exhibits more scatter, as shown by the correlation coefficient of 0.66.

The aseasonal simulation retains similarly strong correlations with TCCON for $X^t_{CH_4}$ and X_{CH_4} (Fig. 4, bottom). Removing the seasonality of emissions also reduces the offset between TCCON and GEOS-Chem $X^t_{CH_4}$ and Northern Hemisphere X_{CH_4}. The northern mid-latitude sites depress the $X^t_{CH_4}$ slope to 0.74 and reduce the goodness of fit of the linear regression, and thus the correlation coefficient, slightly. The scatter about the X_{CH_4} linear regression increases for the Northern Hemisphere sites,

Atmos. Chem. Phys. Discuss., doi:10.5194/acp-2016-303, 2016
Manuscript under review for journal Atmos. Chem. Phys.
Published: 10 May 2016

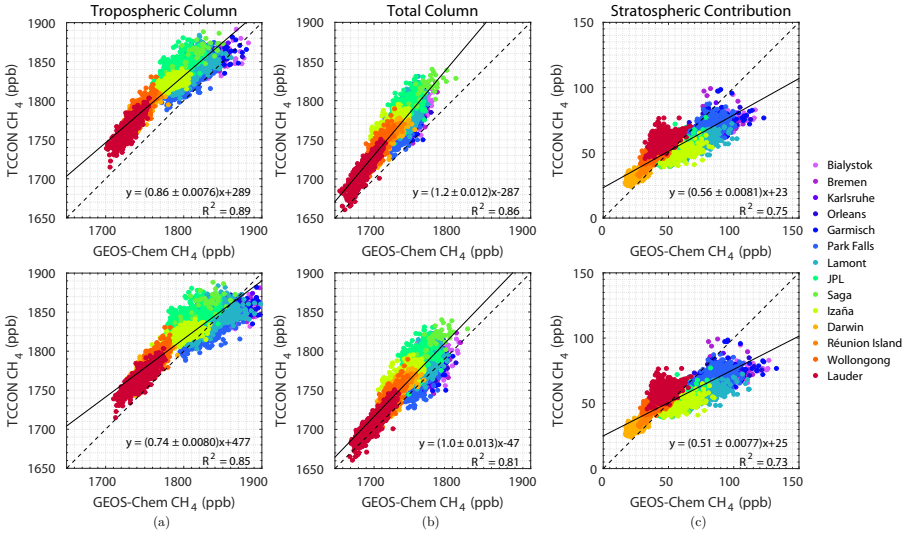

Figure 4. Daily median TCCON and smoothed daily mean GEOS-Chem base (top) and aseasonal (bottom) DMFs for (a) $X^t_{\mathrm{CH_4}}$, (b) $X_{\mathrm{CH_4}}$, and (c) stratospheric contribution. Site colors are as in Fig. 1. Dashed lines mark the one-to-one lines.

but otherwise the fit improves markedly: the slope is 1.0 and the intercept is -47ppb. The stratospheric contribution has nearly the same slope, intercept, and R^2 values as and retains the interhemispheric differences seen in the base simulation.

Figure 5 illustrates how the model differs from ACE-FTS $\mathrm{CH_4}$ measurements in the stratosphere. Excepting the top of the atmosphere in the tropics, $\mathrm{CH_4}$ is considerably lower in the ACE-FTS climatology (v. 2.2, Jones et al., 2012) compared to GEOS-Chem. The difference varies both with altitude and latitude, especially in the Northern spring poleward of $40°\mathrm{N}$. The vertical gradient is the least pronounced in Lauder, where the stratospheric contributions of TCCON and GEOS-Chem agree well (Fig. 4).

3.1 Dependence on Tropopause Height

In the Northern Hemisphere, the measurement-model mismatch of the stratosphere increases as the tropopause altitude shifts downward (Fig. 6). As the stratospheric portion of the total column increases in the model, the error in stratospheric $\mathrm{CH_4}$ produces a larger disagreement with measurements. This introduces both zonal and seasonal biases because the tropopause height decreases with latitude, and this gradient increases during winter and spring. As the effective tropopause, the pressure level at which the model divides the troposphere from the stratosphere in GEOS-Chem, is defined at discrete grid level pressure boundaries, the disagreement exhibits a large spread for relatively few tropopause pressure heights.

The tropospheric mismatch ($\Delta X^t_{\mathrm{CH_4}}$) shows a much weaker correlation to tropopause height, as the upper troposphere is generally well-mixed and chemical loss does not vary with altitude as much as in the lower stratosphere. The slope is dominated by high-latitude sites; the subtropical sites exhibit a much weaker correlation. At Izaña, which is in the sub-tropics at an altitude of 2.4 km, the correlation between $\Delta X^t_{\mathrm{CH_4}}$ and tropopause pressure is weak: the slope of -0.034 ± 0.028 is nearly flat within

Atmos. Chem. Phys. Discuss., doi:10.5194/acp-2016-303, 2016
Manuscript under review for journal Atmos. Chem. Phys.
Published: 10 May 2016

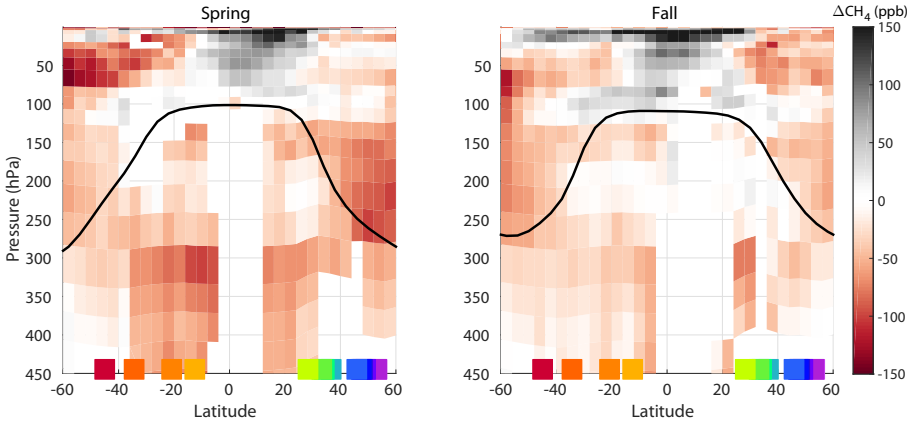

Figure 5. Zonally averaged ACE minus GEOS-Chem climatological CH_4 mole fractions for boreal spring and fall. Black line represents the mean zonal tropopause level. Site colors of squares on the x-axis are as in Fig. 1.

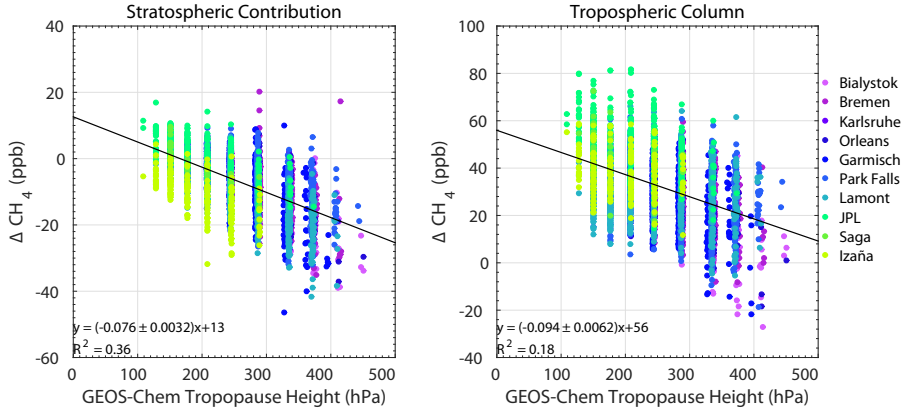

Figure 6. TCCON minus GEOS-Chem CH_4 DMFs as a function of the effective GEOS-Chem tropopause height, shown for Northern Hemisphere sites. Site colors are as in Fig. 1.

error, and R^2 is 0.028. By contrast, the stratospheric relationship at Izaña corresponds within error with the other Northern Hemisphere sites: the slope is -0.087 ± 0.015, and $R^2 = 0.39$. This weaker relationship also demonstrates that the choice of tropopause used in the tropospheric profile integration does not govern $\Delta X^t_{CH_4}$.

3.2 Seasonal Agreement

$\Delta X^t_{CH_4}$ has a periodic trend, indicating that the model error has a strong seasonal component in the troposphere. To isolate stable seasonal patterns from the cumulative influence of emissions, we calculate the detrended seasonal mean DMFs. In the Southern Hemisphere, the measurements and model agree well. Across the Northern Hemisphere sites, however, the seasonality differs (Fig. 7). The seasonal amplitude of GEOS-Chem $X^t_{CH_4}$ is about equal to that of TCCON, but the phase trails TCCON

Atmos. Chem. Phys. Discuss., doi:10.5194/acp-2016-303, 2016
Manuscript under review for journal Atmos. Chem. Phys.
Published: 10 May 2016

Atmospheric Chemistry and Physics Discussions

by two to three months. The TCCON $X^t_{CH_4}$ seasonal minimum is in June/July while the GEOS-Chem seasonal minimum is in September/October. Additionally, while TCCON $X^t_{CH_4}$ begins to decrease in January, GEOS-Chem shows some persistence into the spring.

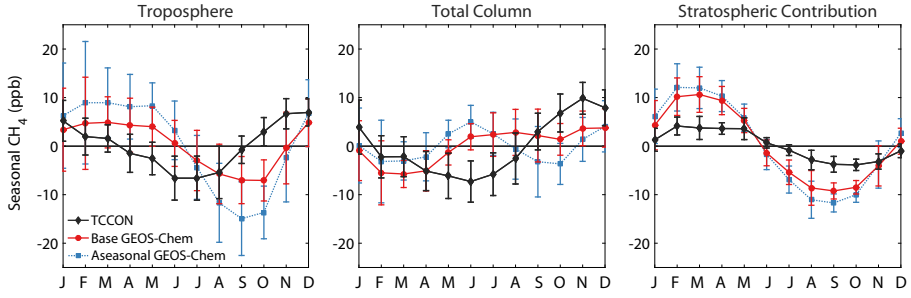

Figure 7. Detrended seasonality of TCCON (black diamonds), GEOS-Chem base (red circles), and GEOS-Chem aseasonal (blue squares) CH_4 DMFs, averaged across Northern Hemisphere sites. Error bars denote the 1σ standard deviation across sites.

The seasonal delay also appears in comparisons of GEOS-Chem surface CH_4 with NOAA surface flask measurements at the LEF site in Park Falls (Fig. 8). The seasonality of GEOS-Chem's surface is regulated more by production and loss than transport: CH_4 peaks in the summer, when wetland emissions are highest (Fig. 10). This contrasts with the flask measurements, which reach a minimum in the summer (Fig. 8). The seasonality covaries remarkably closely with respect to other features: the late winter decrease, spring persistence, and local minimum in October. The spring plateau lasts twice as long as seen in observations, however, and matches $X^t_{CH_4}$, indicating that feature is not the result of vertical transport between the PBL and free troposphere.

Not surprisingly, a time lag does not occur in the stratosphere; the TCCON stratospheric seasonal amplitude is less than half but in phase with that of GEOS-Chem (Fig. 7). The vertical inconsistency of the seasonality produces unusual features in the model total column. From January through April, the TCCON and GEOS-Chem X_{CH_4} are consistent because the model's bias in the troposphere is balanced by the low tropopause. Starting in May, however, the model diverges from the measurements as the higher tropopause limits the stratosphere's influence, and the phase lag in the troposphere dominates. This balancing effect is also demonstrated by the greater variance across sites in the model $X^t_{CH_4}$ and stratospheric contribution compared to measurements, but about the same variance in X_{CH_4}.

For the aseasonal simulation, the tropospheric seasonal cycle amplitude and variance across sites increase, suggesting that the seasonality of emissions in the base simulation has an ameliorating effect on model error (Fig. 7). The stratospheric contribution does not change, however, further demonstrating that the stratosphere is insensitive to perturbations to Northern Hemisphere emissions.

The impact of a static stratosphere and changing troposphere is to make the seasonality of the aseasonal simulation X_{CH_4} bimodal: the October local minimum in the base simulation becomes a fall absolute minimum. The aseasonal X_{CH_4} agrees with TCCON in late winter, masking the greater disagreement in the troposphere. Notably, the main tropospheric features

Atmos. Chem. Phys. Discuss., doi:10.5194/acp-2016-303, 2016
Manuscript under review for journal Atmos. Chem. Phys.
Published: 10 May 2016

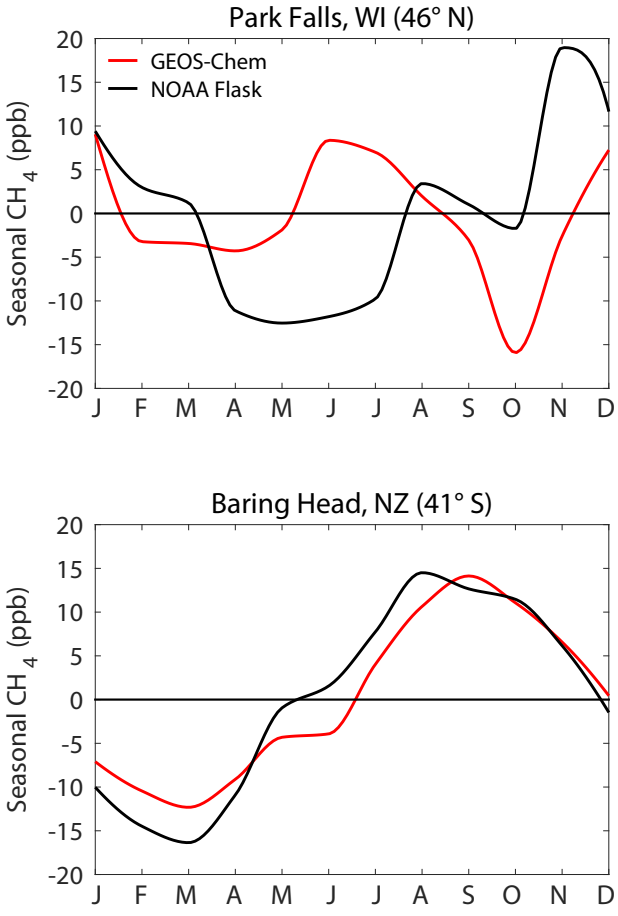

Figure 8. NOAA surface flask (black) and GEOS-Chem surface level (red) seasonality of CH_4 DMFs over 2005-2011 at Park Falls, WI, USA and Baring Head, NZ.

of the base simulation, the seasonal phase lag and spring persistence, are still apparent. OH is not likely the driver of these features, as the Northern Hemisphere phase shift also occurs in simulations performed with large changes in OH (not shown). Transport is thus the most likely driver of these tropospheric trends in the model.

4 Discussion

The stratospheric insensitivity to changes in emissions and tropospheric loss has significant implications for flux inversions. Model inversions use the sensitivity of trace gas concentrations at a given location to perturbations of different emissions sources to adjust those emissions so as to match observations at that location. The model sensitivity kernel implicitly includes uncertainties in transport, chemical loss, and the seasonal and spatial distribution of emissions relative to each other, which are

Atmos. Chem. Phys. Discuss., doi:10.5194/acp-2016-303, 2016
Manuscript under review for journal Atmos. Chem. Phys.
Published: 10 May 2016

Atmospheric Chemistry and Physics Discussions

compounded if vertical levels are subject to different errors. Because the transport errors covary with emissions, they alias into the resulting source attribution.

Comparing measurement and model stratospheric CH_4 as a fraction of the total column provides a normalized comparison that isolates differences in the vertical structure from those caused by initial conditions and unbalanced sources and sinks. Figure 9 illustrates the error associated with the normalized stratospheric column and the associated stratospheric contribution to X_{CH_4} at Park Falls. Although the stratosphere accounts for about 30% of X_{CH_4}, a relatively small error can produce significant seasonal differences; the springtime error of 4×10^{17} molec cm^{-2} (25 ppb) is more than twice the seasonal cycle amplitude. Winter and spring are also when $X^t_{CH_4}$ is least sensitive to seasonal emissions; by contrast, the error is about 15 ppb in the summer, when seasonal emissions have the greatest influence (Fig. 9, top panel). The seasonality of the stratospheric error will therefore distort the inversion mechanism and thus posterior emissions estimates.

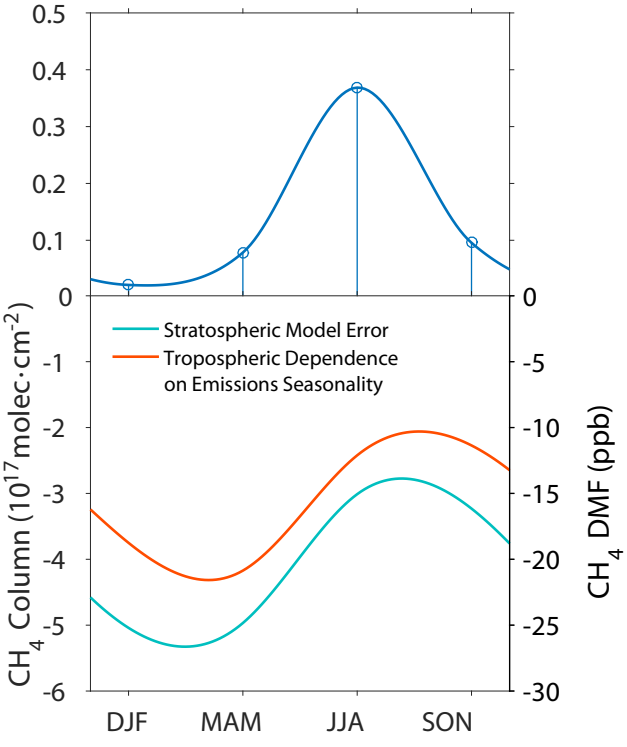

Figure 9. Top: Seasonally-averaged fraction of model emissions from seasonally-varying sources, north of 40°N. Bottom: Seasonally-averaged normalized model stratospheric column error (teal) and the difference between base and aseasonal simulation tropospheric columns (orange) at Park Falls.

Additional bias is introduced by differences in the seasonal patterns of $\Delta X^t_{CH_4}$ and ΔX_{CH_4}. Wetlands are the largest seasonal source of CH_4 in models and the largest natural source in flux inventories, and their emissions are very uncertain. GEOS-Chem CH_4 emissions from northern high-latitude wetlands are extremely variable, with large fluxes in June, July and

Atmos. Chem. Phys. Discuss., doi:10.5194/acp-2016-303, 2016
Manuscript under review for journal Atmos. Chem. Phys.
Published: 10 May 2016

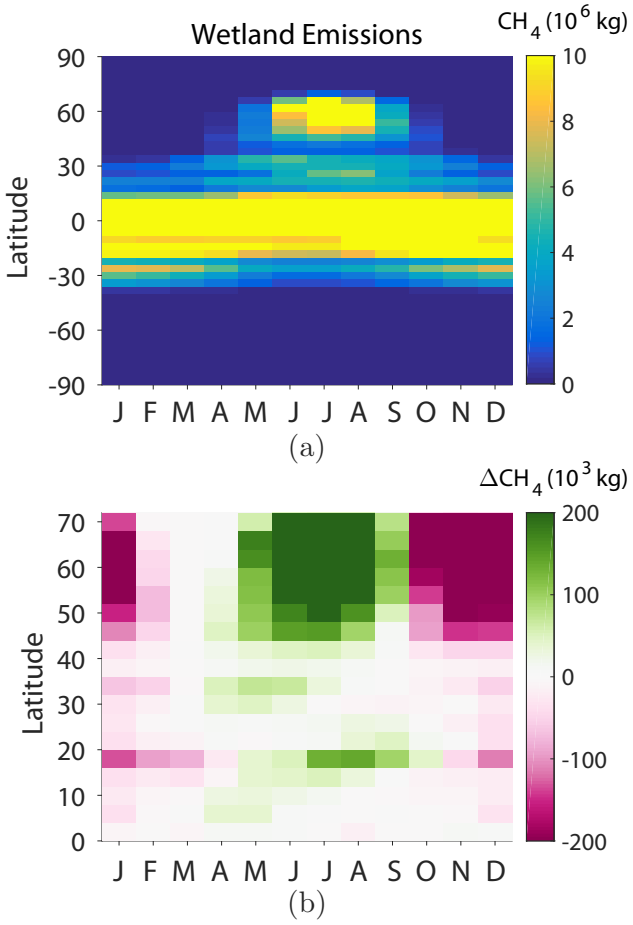

Figure 10. (a) GEOS-Chem monthly zonal mean wetland emissions, in million kg. (b) The Northern Hemisphere sensitivity of GEOS-Chem wetland emission attribution caused by a 3-month lag for each 1 ppb increase of CH_4 at the surface, in thousand kg.

August, moderate fluxes in May and September, and almost no fluxes the remainder of the year (Fig. 10a). Model inversions that scale emissions in a given grid box based on the incorrect seasonality will invariably change the posterior attribution of seasonal emissions. A three-month shift in the troposphere will produce a strong under- or overestimation of posterior wetland fluxes in late spring through early fall. For example, Fig. 10b illustrates the sensitivity of posterior wetland emissions to a three-month lag in the Northern Hemisphere (derived by calculating the total emissions resulting from an increase of 1 ppb of CH_4 in each surface grid box and scaling those emissions according to the a priori contribution of wetlands). The tropics and subtropics are less sensitive to a phase shift, but polewards of $40°$N, both the magnitude and seasonality of the difference is significant. The largest disagreements between measured and modeled $X^t_{CH_4}$ occur when seasonal sources are a small fraction of total emissions, and these seasonal errors will bias source apportionment toward emissions that do not vary on timescales shorter than annually.

Atmos. Chem. Phys. Discuss., doi:10.5194/acp-2016-303, 2016
Manuscript under review for journal Atmos. Chem. Phys.
Published: 10 May 2016

Atmospheric Chemistry and Physics Discussions

5 Conclusions

Assimilation of $X_{\mathrm{CH_4}}$ measurements into global CTMs can help to quantify the global $\mathrm{CH_4}$ budget; however, the treatment of stratospheric chemistry and dynamics must be carefully considered. This work has compared retrieved and modeled $X_{\mathrm{CH_4}}$ and $X^t_{\mathrm{CH_4}}$, parsing out the seasonality of the troposphere and stratosphere and the resulting impacts on $X_{\mathrm{CH_4}}$ (Fig. 9a). While the Southern Hemisphere measurement-model agreement is robust, in the Northern Hemisphere the model's stratospheric contribution is larger, and the mismatch increases as the tropopause height decreases. The result is greater model error at high-latitude sites, with the magnitude of the mismatch varying seasonally. Moreover, GEOS-Chem has a lag in Northern Hemisphere $X^t_{\mathrm{CH_4}}$, which occurs regardless of changes in emissions seasonality and thus seems to be a product of transport errors. Furthermore, the stratosphere is insensitive to changes in the tropospheric emissions or chemical loss. These features smooth the model $X_{\mathrm{CH_4}}$ such that they may agree with total column measurements despite having an incorrect vertical distribution.

Model transport errors coupled with spatial and seasonal measurement sparsity can limit the accuracy of the location and timing of emissions scaling. The differences in the seasonality mismatch across vertical levels amplifies the error uncertainty because the timing of optimized fluxes will be especially susceptible to limitations in model transport. The stronger influence of the stratosphere at higher latitudes due to lower tropopause heights, together with the higher temporal variability of the stratospheric fraction of the total column due to the stronger seasonal cycle of the tropopause, also impacts the seasonality of the meridional gradient.

The influence of stratospheric variability on emissions is not unique to the model chosen for this analysis. Bergamaschi et al. (2013) ran TM5-4DVAR inversions using SCIAMACHY column and NOAA surface measurements and found that the mean biases between the optimized $\mathrm{CH_4}$ profiles and aircraft measurements differ between the PBL, free troposphere, and UTLS. Seasonal emissions from wetlands and biomass burning vary by ± 10 and ± 7 $\mathrm{TgCH_4}$, respectively, from year to year, and the zonal partitioning of posterior emissions is sensitive to the wetland priors chosen. Moreover, the larger changes to emissions and sensitivity to assumptions in the Northern Hemisphere indicate that TM5 is also subject to the strong hemispheric differences found in GEOS-Chem. Ostler et al. (2015) found that ACTM and other CTMs used in TransCom-CH4 are also subject to transport errors that impact emissions optimization. Furthermore, ACTM profiles show a similar over-estimation of stratospheric $\mathrm{CH_4}$, zonally-varying measurement-model mismatch dependent on tropopause height, and a smaller seasonal cycle for Northern Hemisphere $X_{\mathrm{CH_4}}$ compared to TCCON.

In this analysis we have used TCCON $X^t_{\mathrm{CH_4}}$ derived with the HF-proxy method; however, $X^t_{\mathrm{CH_4}}$ calculated using other stratospheric tracers such as nitrous oxide ($\mathrm{N_2O}$) (Wang et al., 2014) would provide an additional constraint on models' representations of the stratosphere, as $\mathrm{N_2O}$ is not subject to the spectral interference with water vapor that impacts HF. Information about the vertical tropospheric $\mathrm{CH_4}$ profile directly retrieved from NDACC spectra (Sepúlveda et al., 2014) can also be used to assess whether transport errors differ at different levels of the free troposphere. Ideally, information from these tropospheric products could be integrated to overcome the limitations of each: the sensitivity of $X^t_{\mathrm{CH_4}}$ to prior assumptions of stratospheric-tropospheric exchange and the sensitivity of profile retrievals to UTLS variability (Ostler et al., 2014).

Atmos. Chem. Phys. Discuss., doi:10.5194/acp-2016-303, 2016
Manuscript under review for journal Atmos. Chem. Phys.
Published: 10 May 2016

Atmospheric Chemistry and Physics Discussions

The insensitivity of model stratospheres to tropospheric change allows for a straightforward solution: prescribed stratospheric CH_4 fields based on satellite observations. As representation of tropical convection and exchange across the UTLS improve in models and reduce stratospheric isolation, chemical loss, and transport mechanisms would need to be improved. The output from more accurate stratospheric models over the time period of interest could be used to set the stratospheric component in the offline CH_4 simulation. For instance, the Universal tropospheric-stratospheric Chemistry eXtension (UCX) mechanism, which has been added to more recent versions of GEOS-Chem, updates the stratospheric component of the standard full chemistry simulation such that CH_4 has more sophisticated upwelling, advection and chemical reaction schemes (Eastham et al., 2014). Models that account for interannual variability in both stratospheric and tropospheric dynamics can then assimilate total column measurements to develop more accurate global CH_4 budgets.

Appendix A: GEOS-Chem Simulations

A1 Equilibrium Sensitivity Experiments

All equilibrium runs for a given simulation have identical meteorology, emissions, and OH fields over June 2004-May 2005. Initial conditions for each year are set by the restart files of the previous run. To calculate columns at each site, GEOS-Chem monthly mean mole fractions are adjusted for the monthly medians of the site's daily mean surface pressures and smoothed with the monthly median scaled prior profiles and averaging kernels, interpolated using the monthly median solar zenith angle daily means. Because Park Falls and Lauder are the only TCCON sites that had started taking measurements over this time period, they are the only sites used to generate smoothed columns for the comparisons to the experimental simulations.

Emissions in the aseasonal simulation were derived by running a two-dimensional regression on the annual emissions to determine the scale factors that would produce the smallest residual of total emissions and the interhemispheric gradient. Figure 11 illustrates the difference in total emissions between the base and aseasonal simulations for each zonal band.

A2 Derivation of Dry Gas Values

Versions of GEOS-Chem prior to v.10 have inconsistencies in wet versus dry definitions of pressure, temperature, and air mass, which propagate into model diagnostics and conversions calculated using these terms. As a consequence, CH_4 concentrations are output assuming air masses that include water vapor but calculated with the molar mass of dry air. For all comparisons in this analysis CH_4 DMFs are calculated taking into account the GEOS-5 specific humidity, SPHU (in units of g_{H2O}/kg_{air}), such that

$$\chi_{CH_4,dry} = \frac{\chi_{CH_4}}{1 - SPHU \times 10^{-3}} \tag{A1}$$

where χ_{CH_4} is the model profile in mole fractions. Dry air profiles were derived by subtracting the water vapor mole fraction, also calculated from the GEOS-5 specific humidity, from the total air mass at each pressure level, as in Wunch et al. (2010); Geibel et al. (2012).

Atmos. Chem. Phys. Discuss., doi:10.5194/acp-2016-303, 2016
Manuscript under review for journal Atmos. Chem. Phys.
Published: 10 May 2016

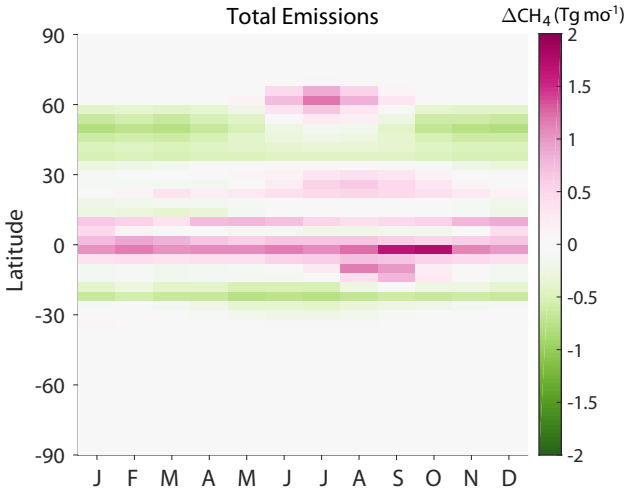

Figure 11. Monthly averages of the difference in total CH_4 emissions between the base and aseasonal GEOS-Chem simulations, in Tg.

A3 Model Smoothing for Measurement Comparisons

Base and aseasonal daily runs were initialized using CH_4 fields from their respective 34th equilibrium cycles. Daily CH_4 mole fractions averaged over both 24-hour and 10-14 local time were output to test whether TCCON's daytime-only observations would introduce a bias in the comparisons. Measurement-model differences were not sensitive to averaging times. Comparison of measurements to model columns produced using the 24-hour and 10-14 local time averages produce equivalent slopes and only slightly different intercepts and correlation coefficients. The seasonality of 10-14 local time DMFs does not differ, except that the fall seasonal maximum of the adjusted troposphere and stratospheric contribution at Park Falls in October, one month later than the 24-hour DMF seasonality.

CH_4 dry vertical profiles for each grid box associated with a TCCON site, $\boldsymbol{x}^{\boldsymbol{m}}_{\mathbf{CH_4}}$, were smoothed with corresponding FTS column averaging kernels, $\boldsymbol{a}_{\mathbf{CH_4}}$, and scaled priors for each day and vertically integrated using pressure-weighted levels:

$$\chi^{s}_{\mathrm{CH_4}} = \gamma_{\mathrm{CH_4}} \cdot \chi^{a}_{\mathrm{CH_4}} + \boldsymbol{a}^{\S}_{\mathbf{CH_4}}(\boldsymbol{x}^{\boldsymbol{m}}_{\mathbf{CH_4}} - \gamma_{\mathrm{CH_4}}\boldsymbol{x}^{\boldsymbol{a}}_{\mathbf{CH_4}}) \tag{A2}$$

where $\chi^{s}_{\mathrm{CH_4}}$ is the smoothed GEOS-Chem column-averaged DMF, $\gamma_{\mathrm{CH_4}}$ is the TCCON daily median retrieved profile scaling factor, and $\boldsymbol{x}^{\boldsymbol{a}}_{\mathbf{CH_4}}$ and $\chi^{a}_{\mathrm{CH_4}}$ are respectively the a priori profile and column-integrated CH_4 DMFs (Rodgers and Connor, 2003). The pressure weighting function, $\boldsymbol{h}$, was applied such that $\chi = \boldsymbol{h}^T\boldsymbol{x}$. TCCON priors were interpolated to the GEOS-Chem pressure grid, and GEOS-Chem pressure and corresponding gas profiles were adjusted using daily mean surface pressures local to each site (Wunch et al., 2010; Messerschmidt et al., 2011). The averaging kernels were interpolated for the local daily mean solar zenith angle and the GEOS-Chem pressure grid so that it could be applied to the difference between the GEOS-Chem and TCCON profiles as $\boldsymbol{a}^{\S}\boldsymbol{x} = \sum_{i=1}^{N} a_i h_i x_i$ from the surface to the highest level, N, at i pressure levels (Connor et al., 2008; Wunch et al., 2011b). Figure 12 shows how the smoothed column compares to the column that only uses the dry gas correction.

Atmos. Chem. Phys. Discuss., doi:10.5194/acp-2016-303, 2016
Manuscript under review for journal Atmos. Chem. Phys.
Published: 10 May 2016

Acknowledgements. Support for this research is provided by the NASA Earth and Space Science Fellowship Program and NASA's Carbon Cycle Science program. Park Falls, Lamont, and JPL are funded by NASA grants NNX14AI60G, NNX11AG01G, NAG5-12247, NNG05-GD07G, and NASA Orbiting Carbon Observatory Program; we are grateful to the DOE ARM program and Jeff Ayers for their technical support in Lamont and Park Falls, respectively. Darwin and Wollongong are funded by NASA grants NAG5-12247 and NNG05-GD07G and the Australian Research Council grants DP140101552, DP110103118, DP0879468 and LP0562346, and Nicholas Deutscher is supported by an Australian Research Council Fellowship, DE140100178; we are grateful to the DOE ARM program for technical support in Darwin. Bremen, Bialystok, and Orleans are funded by the EU projects InGOS and ICOS-INWIRE and by the Senate of Bremen. Réunion Island is funded by the EU FP7 project ICOS-INWIRE, the national Belgian support to ICOS and the AGACC-II project (Science for Sustainable Development Program), the Université de la Réunion, and the French regional and national organizations (INSU, CNRS). From 2004 to 2011 the Lauder TCCON program was funded by the New Zealand Foundation of Research Science and Technology contracts CO1X0204, CO1X0703 and CO1X0406. We thank Shuji Kawakami for his technical support in Saga. We thank Peter Bernath and Chris Boone for their guidance using the ACE-FTS data, which were obtained through the Atmospheric Chemistry Experiment (ACE) mission, primarily funded by the Canadian Space Agency. We are grateful to Geoff Toon for his continuous efforts developing the GGG software, as well as his input on the manuscript. We thank Arlyn Andrews for providing the LEF surface flask data, which were generated by NOAA-ESRL, Carbon Cycle Greenhouse Gases Group. Baring Head NIWA surface data were provided courtesy of Gordon Brailsford, Dave Lowe and Ross Martin. We are grateful to Kelvin Bates for providing monthly OH fields for the GEOS-Chem Updated OH sensitivity experiments.

Atmos. Chem. Phys. Discuss., doi:10.5194/acp-2016-303, 2016
Manuscript under review for journal Atmos. Chem. Phys.
Published: 10 May 2016

References

Baker, D., Law, R., Gurney, K., Rayner, P., Peylin, P., Denning, A., Bousquet, P., Bruhwiler, L., Chen, Y., Ciais, P., Fung, I., Heimann, M., John, J., Maki, T., Maksyutov, S., Masarie, K., Prather, M., Pak, B., Taguchi, S., and Zhu, Z.: TransCom 3 inversion intercomparison: Impact of transport model errors on the interannual variability of regional CO2 fluxes, 1988-2003, Global Biogeochemical Cycles, 20, doi:10.1029/2004GB002439, 2006.

Bergamaschi, P., Frankenberg, C., Meirink, J. F., Krol, M., Dentener, F., Wagner, T., Platt, U., Kaplan, J. O., Körner, S., Heimann, M., Dlugokencky, E. J., and Goede, A.: Satellite chartography of atmospheric methane from SCIAMACHY on board ENVISAT: 2. Evaluation based on inverse model simulations, Journal of Geophysical Research: Atmospheres, 112, n/a–n/a, doi:10.1029/2006JD007268, http://dx.doi.org/10.1029/2006JD007268, d02304, 2007.

Bergamaschi, P., Houweling, S., Segers, A., Krol, M., Frankenberg, C., Scheepmaker, R. A., Dlugokencky, E., Wofsy, S. C., Kort, E. A., Sweeney, C., Schuck, T., Brenninkmeijer, C., Chen, H., Beck, V., and Gerbig, C.: Atmospheric CH4 in the first decade of the 21st century: Inverse modeling analysis using SCIAMACHY satellite retrievals and NOAA surface measurements, Journal of Geophysical Research: Atmospheres, 118, 7350–7369, doi:10.1002/jgrd.50480, http://dx.doi.org/10.1002/jgrd.50480, 2013.

Bernath, P. F.: Atmospheric Chemistry Experiment (ACE): Mission overview, Geophysical Research Letters, 32, L15S01, doi:10.1029/2005GL022386, http://doi.wiley.com/10.1029/2005GL022386, 2005.

Bey, I., Jacob, D., Yantosca, R., Logan, J., Field, B., Fiore, A., Li, Q., Liu, H., Mickley, L., and Schultz, M.: Global modeling of tropospheric chemistry with assimilated meteorology: Model description and evaluation, Journal of Geophysical Research-Atmospheres, 106, 23 073–23 095, doi:10.1029/2001JD000807, 2001.

Boering, K. A., Hintsa, E. J., Wofsy, S. C., Anderson, J. G., Daube, B. C., Dessler, A. E., Loewenstein, M., McCormick, M. P., Podolske, J. R., Weinstock, E. M., and Yue, G. K.: Measurements of stratospheric carbon dioxide and water vapor at northern midlatitudes: Implications for troposphere-to-stratosphere transport, Geophysical Research Letters, 22, 2737–2740, doi:10.1029/95GL02337, http://dx.doi.org/10.1029/95GL02337, 1995.

Butz, A., Galli, A., Hasekamp, O., Landgraf, J., Tol, P., and Aben, I.: {TROPOMI} aboard Sentinel-5 Precursor: Prospective performance of {CH4} retrievals for aerosol and cirrus loaded atmospheres, Remote Sensing of Environment, 120, 267 – 276, doi:http://dx.doi.org/10.1016/j.rse.2011.05.030, http://www.sciencedirect.com/science/article/pii/S003442571200082X, the Sentinel Missions - New Opportunities for Science, 2012.

Connor, B. J., Boesch, H., Toon, G., Sen, B., Miller, C., and Crisp, D.: Orbiting Carbon Observatory: Inverse method and prospective error analysis, Journal of Geophysical Research, 113, 1–14, doi:10.1029/2006JD008336, 2008.

De Mazière, M., Vigouroux, C., Bernath, P. F., Baron, P., Blumenstock, T., Boone, C., Brogniez, C., Catoire, V., Coffey, M., Duchatelet, P., Griffith, D., Hannigan, J., Kasai, Y., Kramer, I., Jones, N., Mahieu, E., Manney, G. L., Piccolo, C., Randall, C., Robert, C., Senten, C., Strong, K., Taylor, J., Tétard, C., Walker, K. A., and Wood, S.: Validation of ACE-FTS v2.2 methane profiles from the upper troposphere to the lower mesosphere, Atmospheric Chemistry and Physics, 8, 2421–2435, doi:10.5194/acp-8-2421-2008, http://www.atmos-chem-phys.net/8/2421/2008/, 2008.

Dlugokencky, E. J., Nisbet, E. G., Fisher, R., and Lowry, D.: Global atmospheric methane: budget, changes and dangers, Philosophical Transactions of the Royal Society of London A: Mathematical, Physical and Engineering Sciences, 369, 2058–2072, doi:10.1098/rsta.2010.0341, http://rsta.royalsocietypublishing.org/content/369/1943/2058, 2011.

Eastham, S. D., Weisenstein, D. K., and Barrett, S. R.: Development and evaluation of the unified tropospheric–stratospheric chemistry extension (UCX) for the global chemistry-transport model GEOS-Chem, Atmospheric Environment, 89, 52–63, doi:http://dx.doi.org/10.1016/j.atmosenv.2014.02.001, http://www.sciencedirect.com/science/article/pii/S1352231014000971, 2014.

Fraser, A., Chan Miller, C., Palmer, P. I., Deutscher, N. M., Jones, N. B., and Griffith, D. W. T.: The Australian methane budget: Interpreting surface and train-borne measurements using a chemistry transport model, Journal of Geophysical Research: Atmospheres, 116, n/a–n/a, doi:10.1029/2011JD015964, http://dx.doi.org/10.1029/2011JD015964, d20306, 2011.

Fraser, A., Palmer, P. I., Feng, L., Boesch, H., Cogan, A., Parker, R., Dlugokencky, E. J., Fraser, P. J., Krummel, P. B., Langenfelds, R. L., O'Doherty, S., Prinn, R. G., Steele, L. P., van der Schoot, M., and Weiss, R. F.: Estimating regional methane surface fluxes: the relative importance of surface and GOSAT mole fraction measurements, Atmospheric Chemistry and Physics, 13, 5697–5713, doi:10.5194/acp-13-5697-2013, http://www.atmos-chem-phys.net/13/5697/2013/, 2013.

Geibel, M. C., Messerschmidt, J., Gerbig, C., Blumenstock, T., Chen, H., Hase, F., Kolle, O., Lavrič, J. V., Notholt, J., Palm, M., Rettinger, M., Schmidt, M., Sussmann, R., Warneke, T., and Feist, D. G.: Calibration of column-averaged CH_4 over European TCCON FTS sites with airborne in-situ measurements, Atmospheric Chemistry and Physics, 12, 8763–8775, doi:10.5194/acp-12-8763-2012, http://www.atmos-chem-phys.net/12/8763/2012/, 2012.

Gentner, D. R., Ford, T. B., Guha, A., Boulanger, K., Brioude, J., Angevine, W. M., de Gouw, J. A., Warneke, C., Gilman, J. B., Ryerson, T. B., Peischl, J., Meinardi, S., Blake, D. R., Atlas, E., Lonneman, W. A., Kleindienst, T. E., Beaver, M. R., St Clair, J. M., Wennberg, P. O., VandenBoer, T. C., Markovic, M. Z., Murphy, J. G., Harley, R. A., and Goldstein, A. H.: Emissions of organic carbon and methane from petroleum and dairy operations in California's San Joaquin Valley, Atmospheric Chemistry and Physics, 14, 4955–4978, doi:10.5194/acp-14-4955-2014, 2014.

Jones, A., Walker, K. A., Jin, J. J., Taylor, J. R., Boone, C. D., Bernath, P. F., Brohede, S., Manney, G. L., McLeod, S., Hughes, R., and Daffer, W. H.: Technical Note: A trace gas climatology derived from the Atmospheric Chemistry Experiment Fourier Transform Spectrometer (ACE-FTS) data set, Atmospheric Chemistry and Physics, 12, 5207–5220, doi:10.5194/acp-12-5207-2012, http://www.atmos-chem-phys.net/12/5207/2012/, 2012.

Mahieu, E., Duchatelet, P., Demoulin, P., Walker, K. A., Dupuy, E., Froidevaux, L., Randall, C., Catoire, V., Strong, K., Boone, C. D., Bernath, P. F., Blavier, J.-F., Blumenstock, T., Coffey, M., De Mazière, M., Griffith, D., Hannigan, J., Hase, F., Jones, N., Jucks, K. W., Kagawa, A., Kasai, Y., Mebarki, Y., Mikuteit, S., Nassar, R., Notholt, J., Rinsland, C. P., Robert, C., Schrems, O., Senten, C., Smale, D., Taylor, J., Tétard, C., Toon, G. C., Warneke, T., Wood, S. W., Zander, R., and Servais, C.: Validation of ACE-FTS v2.2 measurements of HCl, HF, CCl_3F and CCl_2F_2 using space-, balloon- and ground-based instrument observations, Atmospheric Chemistry and Physics, 8, 6199–6221, doi:10.5194/acp-8-6199-2008, http://www.atmos-chem-phys.net/8/6199/2008/, 2008.

Messerschmidt, J., Geibel, M. C., Blumenstock, T., Chen, H., Deutscher, N. M., Engel, A., Feist, D. G., Gerbig, C., Gisi, M., Hase, F., Katrynski, K., Kolle, O., Lavrič, J. V., Notholt, J., Palm, M., Ramonet, M., Rettinger, M., Schmidt, M., Sussmann, R., Toon, G. C., Truong, F., Warneke, T., Wennberg, P. O., Wunch, D., and Xueref-Remy, I.: Calibration of TCCON column-averaged CO_2: the first aircraft campaign over European TCCON sites, Atmospheric Chemistry and Physics, 11, 10 765–10 777, doi:10.5194/acp-11-10765-2011, http://www.atmos-chem-phys.net/11/10765/2011/, 2011.

Ostler, A., Sussmann, R., Rettinger, M., Deutscher, N. M., Dohe, S., Hase, F., Jones, N., Palm, M., and Sinnhuber, B.-M.: Multistation intercomparison of column-averaged methane from NDACC and TCCON: impact of dynamical variability, Atmospheric Measurement Techniques, 7, 4081–4101, doi:10.5194/amt-7-4081-2014, http://www.atmos-meas-tech.net/7/4081/2014/, 2014.

Ostler, A., Sussmann, R., Patra, P. K., Wennberg, P. O., Deutscher, N. M., Griffith, D. W. T., Blumenstock, T., Hase, F., Kivi, R., Warneke, T., Wang, Z., De Mazière, M., Robinson, J., and Ohyama, H.: The imprint of stratospheric transport on column-averaged methane, doi:10.5194/acpd-15-20395-2015, http://www.atmos-chem-phys-discuss.net/15/20395/2015/, 2015.

Parker, R., Boesch, H., Cogan, A., Fraser, A., Feng, L., Palmer, P. I., Messerschmidt, J., Deutscher, N., Griffith, D. W. T., Notholt, J., Wennberg, P. O., and Wunch, D.: Methane observations from the Greenhouse Gases Observing SATellite: Comparison to ground-based TCCON data and model calculations, Geophysical Research Letters, 38, n/a–n/a, doi:10.1029/2011GL047871, http://dx.doi.org/10.1029/2011GL047871, l15807, 2011.

Patra, P. K., Houweling, S., Krol, M., Bousquet, P., Belikov, D., Bergmann, D., Bian, H., Cameron-Smith, P., Chipperfield, M. P., Corbin, K., Fortems-Cheiney, A., Fraser, A., Gloor, E., Hess, P., Ito, A., Kawa, S. R., Law, R. M., Loh, Z., Maksyutov, S., Meng, L., Palmer, P. I., Prinn, R. G., Rigby, M., Saito, R., and Wilson, C.: TransCom model simulations of CH_4 and related species: linking transport, surface flux and chemical loss with CH_4 variability in the troposphere and lower stratosphere, Atmospheric Chemistry and Physics, 11, 12 813–12 837, doi:10.5194/acp-11-12813-2011, http://www.atmos-chem-phys.net/11/12813/2011/, 2011.

Rodgers, C. D. and Connor, B. J.: Intercomparison of remote sounding instruments, Journal of Geophysical Research, 108, 4116, doi:10.1029/2002JD002299, 2003.

Saad, K. M., Wunch, D., Toon, G. C., Bernath, P., Boone, C., Connor, B., Deutscher, N. M., Griffith, D. W. T., Kivi, R., Notholt, J., Roehl, C., Schneider, M., Sherlock, V., and Wennberg, P. O.: Derivation of tropospheric methane from TCCON CH_4 and HF total column observations, Atmospheric Measurement Techniques, 7, 2907–2918, doi:10.5194/amt-7-2907-2014, http://www.atmos-meas-tech.net/7/2907/2014/, 2014.

Santoni, G. W., Daube, B. C., Kort, E. A., Jimenez, R., Park, S., Pittman, J. V., Gottlieb, E., Xiang, B., Zahniser, M. S., Nelson, D. D., McManus, J. B., Peischl, J., Ryerson, T. B., Holloway, J. S., Andrews, A. E., Sweeney, C., Hall, B., Hintsa, E. J., Moore, F. L., Elkins, J. W., Hurst, D. F., Stephens, B. B., Bent, J., and Wofsy, S. C.: Evaluation of the airborne quantum cascade laser spectrometer (QCLS) measurements of the carbon and greenhouse gas suite - CO2, CH4, N2O, and CO - during the CalNex and HIPPO campaigns, Atmospheric Measurement Techniques, 7, 1509–1526, doi:10.5194/amt-7-1509-2014, 2014.

Sepúlveda, E., Schneider, M., Hase, F., Barthlott, S., Dubravica, D., García, O. E., Gomez-Pelaez, A., González, Y., Guerra, J. C., Gisi, M., Kohlhepp, R., Dohe, S., Blumenstock, T., Strong, K., Weaver, D., Palm, M., Sadeghi, A., Deutscher, N. M., Warneke, T., Notholt, J., Jones, N., Griffith, D. W. T., Smale, D., Brailsford, G. W., Robinson, J., Meinhardt, F., Steinbacher, M., Aalto, T., and Worthy, D.: Tropospheric CH_4 signals as observed by NDACC FTIR at globally distributed sites and comparison to GAW surface in situ measurements, Atmospheric Measurement Techniques, 7, 2337–2360, doi:10.5194/amt-7-2337-2014, http://www.atmos-meas-tech.net/7/2337/2014/, 2014.

Stephens, B. B., Gurney, K. R., Tans, P. P., Sweeney, C., Peters, W., Bruhwiler, L., Ciais, P., Ramonet, M., Bousquet, P., Nakazawa, T., Aoki, S., Machida, T., Inoue, G., Vinnichenko, N., Lloyd, J., Jordan, A., Heimann, M., Shibistova, O., Langenfelds, R. L., Steele, L. P., Francey, R. J., and Denning, A. S.: Weak Northern and Strong Tropical Land Carbon Uptake from Vertical Profiles of Atmospheric CO2, Science, 316, 1732–1735, doi:10.1126/science.1137004, http://science.sciencemag.org/content/316/5832/1732, 2007.

Turner, A. J., Jacob, D. J., Wecht, K. J., Maasakkers, J. D., Lundgren, E., Andrews, A. E., Biraud, S. C., Boesch, H., Bowman, K. W., Deutscher, N. M., Dubey, M. K., Griffith, D. W. T., Hase, F., Kuze, A., Notholt, J., Ohyama, H., Parker, R., Payne, V. H., Sussmann, R., Sweeney, C., Velazco, V. A., Warneke, T., Wennberg, P. O., and Wunch, D.: Estimating global and North American methane emissions with high spatial resolution using GOSAT satellite data, Atmospheric Chemistry and Physics, 15, 7049–7069, doi:10.5194/acp-15-7049-2015, http://www.atmos-chem-phys.net/15/7049/2015/, 2015.

Wang, J., Logan, J., McElroy, M., Duncan, B., Megretskaia, I., and Yantosca, R.: A 3-D model analysis of the slowdown and interannual variability in the methane growth rate from 1988 to 1997, GLOBAL BIOGEOCHEMICAL CYCLES, 18, doi:10.1029/2003GB002180, 2004.

Wang, Z., Deutscher, N. M., Warneke, T., Notholt, J., Dils, B., Griffith, D. W. T., Schmidt, M., Ramonet, M., and Gerbig, C.: Retrieval of tropospheric column-averaged CH_4 mole fraction by solar absorption FTIR-spectrometry using N_2O as a proxy, Atmospheric Measurement Techniques, 7, 3295–3305, doi:10.5194/amt-7-3295-2014, http://www.atmos-meas-tech.net/7/3295/2014/, 2014.

Washenfelder, R. A., Wennberg, P. O., and Toon, G. C.: Tropospheric methane retrieved from ground-based near-IR solar absorption spectra, Geophysical Research Letters, 30, 2226, doi:10.1029/2003GL017969, http://doi.wiley.com/10.1029/2003GL017969http://dx.doi.org/10.1029/2003GL017969, 2003.

Waugh, D. and Hall, T.: Age of Stratospheric Air: Theory, Observations, and Models, Reviews of Geophysics, 40, 1–1–1–26, doi:10.1029/2000RG000101, http://dx.doi.org/10.1029/2000RG000101, 1010, 2002.

Waymark, C., Walker, K., Boone, C., and Bernath, P.: ACE-FTS version 3.0 data set: validation and data processing update, Annals of Geophysics, 56, http://www.annalsofgeophysics.eu/index.php/annals/article/view/6339, 2014.

Wecht, K. J., Jacob, D. J., Frankenberg, C., Jiang, Z., and Blake, D. R.: Mapping of North American methane emissions with high spatial resolution by inversion of SCIAMACHY satellite data, Journal of Geophysical Research: Atmospheres, 119, 7741–7756, doi:10.1002/2014JD021551, http://dx.doi.org/10.1002/2014JD021551, 2014JD021551, 2014a.

Wecht, K. J., Jacob, D. J., Sulprizio, M. P., Santoni, G. W., Wofsy, S. C., Parker, R., Bösch, H., and Worden, J.: Spatially resolving methane emissions in California: constraints from the CalNex aircraft campaign and from present (GOSAT, TES) and future (TROPOMI, geostationary) satellite observations, Atmospheric Chemistry and Physics, 14, 8173–8184, doi:10.5194/acp-14-8173-2014, http://www.atmos-chem-phys.net/14/8173/2014/, 2014b.

Wunch, D., Toon, G. C., Wennberg, P. O., Wofsy, S. C., Stephens, B. B., Fischer, M. L., Uchino, O., Abshire, J. B., Bernath, P., Biraud, S. C., Blavier, J.-F. L., Boone, C., Bowman, K. P., Browell, E. V., Campos, T., Connor, B. J., Daube, B. C., Deutscher, N. M., Diao, M., Elkins, J. W., Gerbig, C., Gottlieb, E., Griffith, D. W. T., Hurst, D. F., Jiménez, R., Keppel-Aleks, G., Kort, E. a., Macatangay, R., Machida, T., Matsueda, H., Moore, F., Morino, I., Park, S., Robinson, J., Roehl, C. M., Sawa, Y., Sherlock, V., Sweeney, C., Tanaka, T., and Zondlo, M. a.: Calibration of the Total Carbon Column Observing Network using aircraft profile data, Atmospheric Measurement Techniques, 3, 1351–1362, doi:10.5194/amt-3-1351-2010, http://www.atmos-meas-tech.net/3/1351/2010/, 2010.

Wunch, D., Toon, G. C., Blavier, J.-F. L., Washenfelder, R. a., Notholt, J., Connor, B. J., Griffith, D. W. T., Sherlock, V., and Wennberg, P. O.: The Total Carbon Column Observing Network, Philosophical transactions. Series A, Mathematical, physical, and engineering sciences, 369, 2087–2112, doi:10.1098/rsta.2010.0240, http://www.ncbi.nlm.nih.gov/pubmed/21502178, 2011a.

Wunch, D., Wennberg, P. O., Toon, G. C., Connor, B. J., Fisher, B., Osterman, G. B., Frankenberg, C., Mandrake, L., O'Dell, C., Ahonen, P., Biraud, S. C., Castano, R., Cressie, N., Crisp, D., Deutscher, N. M., Eldering, a., Fisher, M. L., Griffith, D. W. T., Gunson, M., Heikkinen, P., Keppel-Aleks, G., Kyrö, E., Lindenmaier, R., Macatangay, R., Mendonca, J., Messerschmidt, J., Miller, C. E., Morino, I., Notholt, J., Oyafuso, F. a., Rettinger, M., Robinson, J., Roehl, C. M., Salawitch, R. J., Sherlock, V., Strong, K., Sussmann, R., Tanaka, T., Thompson, D. R., Uchino, O., Warneke, T., and Wofsy, S. C.: A method for evaluating bias in global measurements of CO2 total columns from space, Atmospheric Chemistry and Physics, 11, 12 317–12 337, doi:10.5194/acp-11-12317-2011, http://www.atmos-chem-phys.net/11/12317/2011/acp-11-12317-2011.htmlhttp://www.atmos-chem-phys.net/11/12317/2011/, 2011b.

Wunch, D., Toon, G. C., Sherlock, V., Deutscher, N. M., Liu, C., Feist, D. G., and Wennberg, P. O.: The Total Carbon Column Observing Network's GGG2014 Data Version, Tech. rep., Carbon Dioxide Information Analysis Center, Oak Ridge National Laboratory, Oak Ridge,

Atmos. Chem. Phys. Discuss., doi:10.5194/acp-2016-303, 2016
Manuscript under review for journal Atmos. Chem. Phys.
Published: 10 May 2016

Atmospheric Chemistry and Physics Discussions

Tennessee, U.S.A. doi: 10.14291/tccon.ggg2014.documentation.R0/1221662, doi:10.14291/tccon.ggg2014.documentation.R0/1221662, http://dx.doi.org/10.14291/tccon.ggg2014.documentation.R0/1221662, 2015.

Yang, Z., Washenfelder, R. a., Keppel-Aleks, G., Krakauer, N. Y., Randerson, J. T., Tans, P. P., Sweeney, C., and Wennberg, P. O.: New constraints on Northern Hemisphere growing season net flux, Geophysical Research Letters, 34, L12 807, doi:10.1029/2007GL029742, http://doi.wiley.com/10.1029/2007GL029742, 2007.

Atmos. Chem. Phys. Discuss., doi:10.5194/acp-2016-303, 2016
Manuscript under review for journal Atmos. Chem. Phys.
Published: 10 May 2016

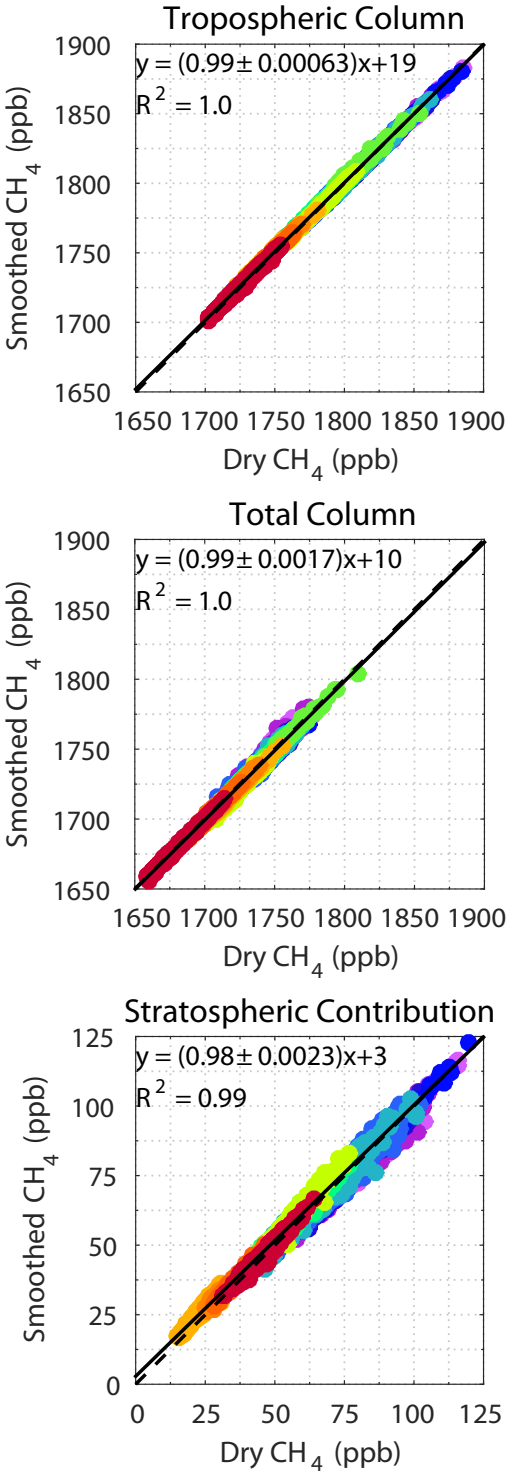

Figure 12. Smoothed versus dry integrated GEOS-Chem CH_4 DMFs for base simulation tropospheric columns, total columns, and stratospheric contribution. Site colors are as in Fig. 1. Dashed lines mark the one-to-one lines.